Metallomics Study of CdSe/ZnS Quantum Dots in HepG2 Cells

Lu Peng, Man He, Beibei Chen, Yu Qiao, and Bin Hu*

Key Laboratory of Analytical Chemistry for Biology and Medicine (Ministry of Education), Department of Chemistry, Wuhan University, Wuhan 430072, PR China

ABSTRACT Toxicity of quantum dots (QDs) has been a hot research concern in the past decade, and there is a lot of challenge in this field. The physicochemical characteristics of QDs can affect their toxicity, while little is known about the specific chemical form of QDs in living cells after incubation so far. In this work, speciation of four CdSe/ZnS QDs in HepG2 cells was carried out from the metallomics' point of view for the first time by using size exclusion chromatography (SEC) coupled with inductively coupled plasma-mass spectrometry (ICP-MS). On the basis of the signal of Cd, two kinds of chemical forms, named as QD-1 and QD-2, were observed in HepG2 cells incubated with CdSe/ZnS QDs. QD-1 was demonstrated to be a kind of QD-like nanoparticles, confirmed by chromatographic retention time, transmission electron microscopy (TEM) characterization, and fluorescence detection. QD-2 was demonstrated to be cadmium–metallothioneins complex (Cd-MTs) by reversed phase liquid chromatography (RPLC) synchronously coupled with ICP-MS and electrospray ionization quadrupole time-of-flight mass spectrometry (ESI-Q-TOF-MS) analysis. Meanwhile, speciation of QDs in HepG2 cells incubated with different conditions was analyzed. With the variation of QDs incubation concentration/time, and elimination time, the species of QD-1 and QD-2 were also observed without other obvious species, and both the amount of QD-1 and QD-2 increased with incubation concentration and time. The obtained results provide valuable information and a strategy for the study of existing chemical form of QDs, greatly benefiting the understanding of QDs toxicity in living cells.

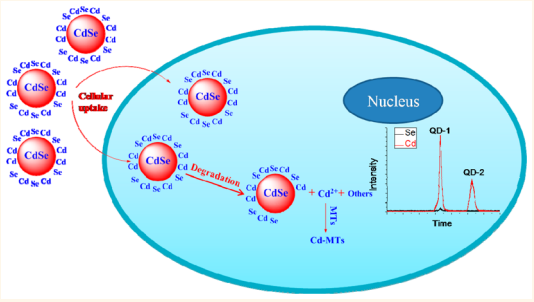

KEYWORDS: CdSe/ZnS quantum dots · speciation · toxicity · metallomics · inductively coupled plasma mass spectrometry · HepG2 cells

Functionalized nanomaterials have been widely used in the fields of electronics, energy, environment and biomedicine as a result of the rapid development of nanotechnology over the past decade. Because of their unique optical properties, quantum dots (QDs) have been considered as a novel fluorescent probe and extensively used in biomedical imaging, cancer diagnostics and drug delivery.[1−3] However, the biosafety of QDs has been a tough question to be answered before the QDs community moves into the clinical application because of their nanosize effect and heavy-metal components.

In recent years, it has been demonstrated that the cytotoxicity of QDs would result in cell morphology and structure variation, cell growth inhibition, mitochondrial dysfunction, DNA damage and apoptosis;[4,5] the physicochemical properties, including the composition, size, surface charge and surface coatings affect the toxicity of QDs to a great extent.[6−10] To further understand and elucidate the toxicity caused by QDs, many research groups have focused their attention on the mechanism study. The production of reactive oxygen species (ROS) and the release of toxic heavy metals have been considered to be the main reason for QDs cytotoxicity.[11−13] Unfortunately, toxicity caused by QDs is extremely complicated and little consensus has been reached. Once exposed to the environmental or biological system, QDs, as well as other nanoparticles, were unlikely to keep their original forms, and the transformation of QDs in cells may be one important reason for the complexity of mechanism. These transformations involve adsorption, chemical reaction, dissolution, decomposition and aggregation, and can affect the uptake, transport, elimination and toxicity of QDs.[14−18] For instance, CdSe QDs might decompose under oxidative and acidic conditions and release Cd.[19−21] At the cellular level, Cd can induce oxidative stress, mitochondrial damage, apoptosis and disrupt the intracellular

* Address correspondence to binhu@whu.edu.cn.

Received for review July 14, 2015 and accepted September 21, 2015.

Published online September 21, 2015
10.1021/acsnano.5b04365

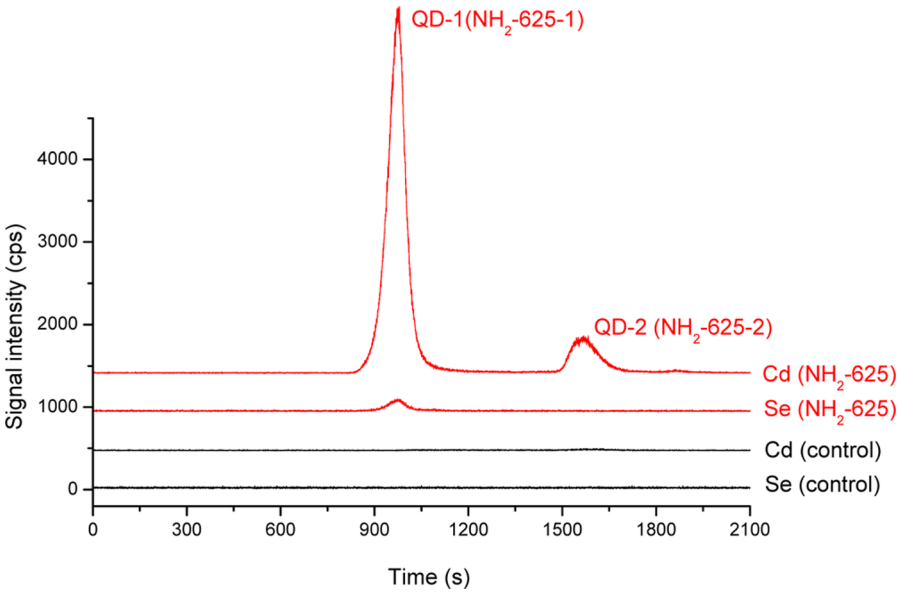

Figure 1. Speciation of QDs in HepG2 cells incubated with (NH_2-625) and without (Control) QDs by SEC-ICP-MS.

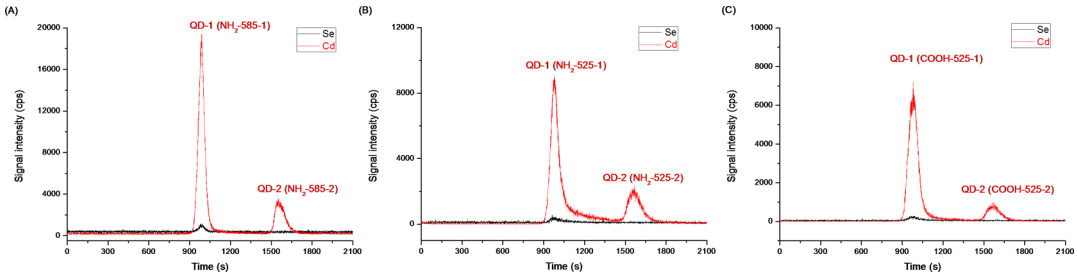

Figure 2. Speciation of QDs in HepG2 cells incubated with QDs determined by SEC-ICP-MS. (A) NH_2-585; (B) NH_2-525; (C) COOH-525.

calcium signaling.[22] The release of Cd from QDs plays a key role in toxicity of QDs. Wiecinski *et al.*[20] studied the toxicity of oxidatively degraded QDs to Zebrafish, and the results indicated that oxidatively weathered QDs showed more toxic to Zebrafish relative to the intact QDs. The increase in toxicity appeared attributable to the oxidative degradation before incubation. Soenen *et al.*[21] found CdSe/CdS QDs rapidly degraded under endosomal pH and release Cd, and the intracellular degradation of QDs was found to augment cytotoxicity with time, resulting in mitochondrial and DNA damage, cell morphology and functionality variation.

The degradation of QDs in living cells were observed by many researchers, but little has been reported on the existing species of QDs after degradation. The metal composition of QDs inspired us to investigate their speciation in cells from metallomics' point of view. Metallomics is a novel omics science which was developed in this decade,[23−25] focusing on the amount, speciation, distribution, structure and function of metals in biological system. It provided a special and efficient insight into the biological effects for metal based nanomaterials (QDs, gold nanoparticles, silver nanoparticles).[26,27] The effective platform for metallomics study presently is hyphenated techniques combining high-resolution separation technique (liquid chromatography, gas chromatography, gel electrophoresis or capillary electrophoresis) with sensitive elemental or molecular mass spectrometry detection. The hyphenated techniques, especially those inductively coupled plasma-mass spectrometry (ICP-MS)-based alternatives have been demonstrated to be effective for the speciation of nanoparticles. For instance, the liquid chromatography techniques, including size exclusion chromatograph (SEC) and reverse-phase high performance liquid chromatography (RPLC), coupled with ICP-MS techniques have been successfully applied for separating species of Au nanoparticles and QDs in aqueous solution.[28−31]

In this work, the speciation of four CdSe/ZnS QDs in HepG2 cells was achieved by using ICP-MS-based hyphenated techniques. The existing species of QDs in the incubated HepG2 cells were fractionated by SEC-ICP-MS first and characterized by parallel RPLC-ICP-MS/electrospray ionization quadrupole time-of-flight mass spectrometry (ESI-Q-TOF-MS), transmission electron microscopy (TEM), and fluorescent spectrometry.

Meanwhile, the effect of the incubation concentrations, incubation time and elimination time on the speciation of QDs was evaluated in detail.

RESULTS

Speciation of CdSe/ZnS QDs in HepG2 Cells by SEC-ICP-MS. The species of QDs in HepG2 cells was analyzed by SEC-ICP-MS. Two distinct peaks were observed in HepG2 cells incubated with CdSe/ZnS QDs by determining Cd. These two peaks with retention time (t_R) at 975s and 1565s were denoted as QD-1 and QD-2, respectively (Figure 1). For NH_2-625 QD group, QD-1 and QD-2 were named as NH_2-625-1 and NH_2-625-2, respectively. The other three groups (NH_2-585, NH_2-525, COOH-525) referred to the same naming rule (Figure 2). In the control group, no obvious signal was found. This suggested the QD-1 and QD-2 were formed as the result of cellular uptake of CdSe/ZnS QDs.

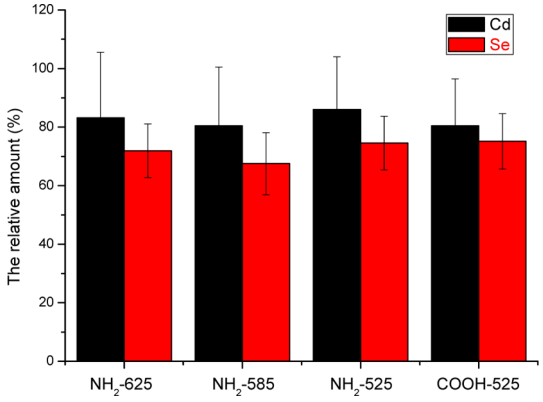

Figure 3. Relative amount of Cd/Se in QD-1 and QD-2 compared with the total amount of QDs in HepG2 cells. The total amount of QDs was set as 100%.

The amount of Cd and Se in QD-1 and QD-2, and inside the cells after incubation were determined, respectively, and the results are shown in Figure 3. As can be seen, the amount of Cd/Se in QD-1 and QD-2 *vs* that in the cells were both higher than 70%, suggesting that the QDs ingested by the cells mainly existed as QD-1 and QD-2, and the proportion of undetected species in the total amount of ingested QDs was very low. Meanwhile, cadmium-ethylenediamine tetraacetic acid (Cd-EDTA), as the representative of small molecular Cd complex, was analyzed by SEC-ICP-MS and appeared at 1860s (t_R). However, no peaks at this time point were found in HepG2 cells incubated with all QDs, indicating that no small molecule Cd-complex detected in HepG2 cells incubated with CdSe/ZnS QDs.

Characterization of QD-1. The QD-1 species contained both Cd and Se as shown in Figure 1 and according to the t_R of standard BSA protein (1134s), the molecular weight of QD-1 (975s) was larger than 68KDa. Thus, it is assumed that QD-1 was a macromolecule complex. For a comparison, the retention performance of original QDs and QD-1 was analyzed by SEC-ICP-MS. As shown in Figure 4A, the retention time of NH_2-625-1 (975s) was close to that of NH_2-625 QDs (980s) by determining Cd and Se, suggesting a similar retention performance for them. The other three QDs group showed the similar results (Figure 4B–D), as the t_R of NH_2-585-1 (978s), NH_2-525-1 (977s) and COOH-525-1 (980s), was close to that of NH_2-585 QD (980s), NH_2-525 QD (982s) and COOH-525 QD (985s), respectively.

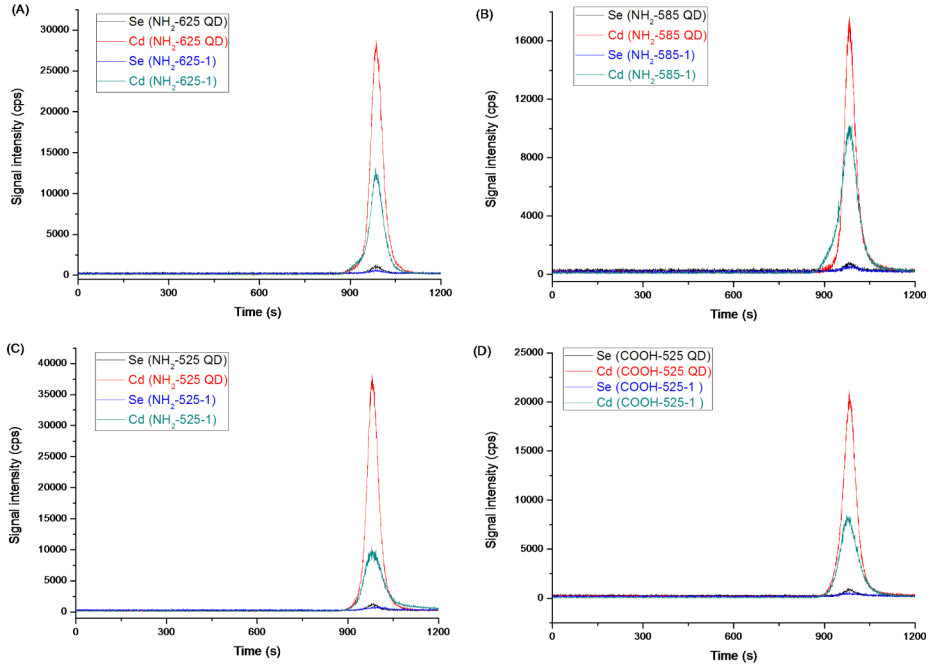

Figure 4. Retention time of QD-1 and original QDs obtained by SEC-ICP-MS. (A) NH_2-625; (B) NH_2-585; (C) NH_2-525; (D) COOH-525.

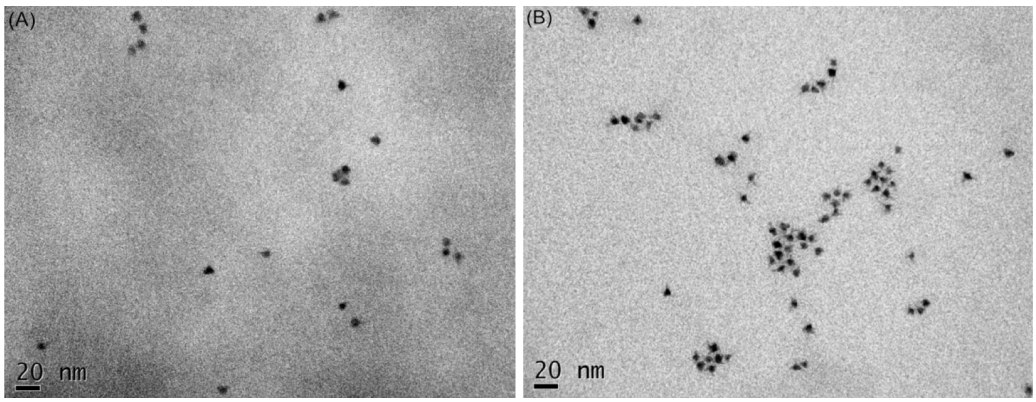

Figure 5. TEM photograph of NH_2-625-1 (A) and NH_2-625 QD (B).

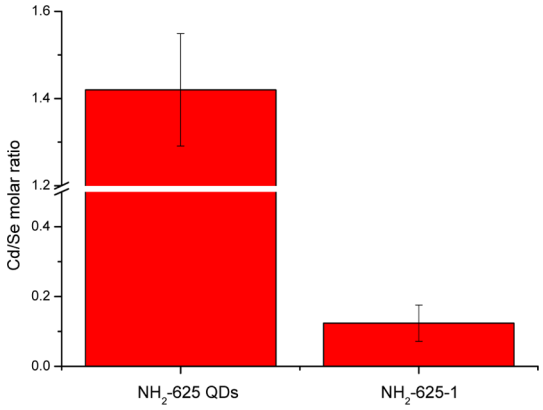

Figure 6. Molar ratio of Cd and Se in NH_2-625 QD and NH_2-625-1.

To further verify whether QD-1 was a kind of nanoparticle or other macromolecule complex, the morphology of NH_2-625-1, as a representative of QD-1, was characterized by TEM. The results in Figure 5A confirmed that NH_2-625-1 was a kind of nanoparticles with a similar size to NH_2-625 QDs (Figure 5B). However, the molar ratio of Cd and Se in QD-1 was significantly lower than that in the NH_2-625 QDs (Figure 6). Meanwhile, the fluorescence properties of QD-1 and original QDs were investigated and compared. As shown in Figure 7A, the maximum emission of NH_2-625 QDs was 619 nm, but no emission peak was found in NH_2-625-1 sample in the same scan range. The other three QD-1 (NH_2-585-1, NH_2-525-1, COOH-525-1) showed the similar results without any emission peak in QD-1 (Figure 7B–D). From the results as shown in Figure 4–7, it can be deduced that QD-1 species is kind of nanoparticles consisting of Cd and Se which has a similar size but different Cd/Se ratio to the original QDs form. Therefore, we concluded the QD-1 species was a kind of QD-like nanoparticles, which might contain both original and degraded QDs.

Characterization of QD-2. The retention performance of two kinds of Cd- metallothioneins (MTs) (Cd-MT1 and Cd-MT2 standards) was investigated by SEC-ICP-MS. As shown in Figure 8, the t_R of NH_2-625-2 (1565s) was between that of Cd-MT1 (1540s) and Cd-MT2 (1585s), suggesting QD-2 was a small molecule complex with a molecular weight of 6000–7000 Da. The results of other three QDs groups were similar and all the t_R of QD-2 species were between 1540s and 1585s (Figure 8).

To further confirm whether the QD-2 is a kind of metallothionein (MT), a hyphenated technique coupling RPLC with ICP-MS and ESI-Q-TOF-MS synchronously was established. The NH_2-625-2 species was analyzed as the representative of QD-2. The result of ICP-MS showed a signal of Cd and Zn (Figure 9). At the time point of 1170s, ESI-Q-TOF-MS results showed a signal of MTs containing Cd and Zn. Meanwhile, the signal of demetalated-metallothioneins (apo-MTs) was found after postcolumn acidification. The detailed MS information on NH_2-625-2 is listed in Table 1. Two kinds of apo-MTs, MT1m and N-terminal acetylation MT2a (N Ac-MT2a), and four kinds of MTs containing Cd and Zn were found, including Cd_6Zn–N Ac-MT2a, Cd_5Zn_2–N Ac-MT2a, Cd_6Zn-MT1m and Cd_5Zn_2-MT1m. The measured mass accuracy of all MTs was less than 10 ppm. The detailed mass spectra of MTs and apo-MTs are shown in Figure S1. The MS results confirmed that QD-2 was a kind of Cd containing MTs.

Speciation of CdSe/ZnS QDs in HepG2 Cells Incubated with Different Concentrations. HepG2 cells were incubated with different concentrations of QDs (10, 50, 100 nM) for 24 h, and the speciation of QDs were analyzed by SEC-ICP-MS. As shown in Figure 10A, only two species, QD-1 and QD-2, were found in HepG2 cells incubated with NH_2-625 QD under different concentrations. But the amount of QD-1 and QD-2 (as Cd) both increased with the increase of the incubation concentration. The same tendency was observed by determining Se signal as shown in Figure 10B. Meanwhile, the amount ratio of Cd and Se in QD-1 was determined by ICP-MS and the results are shown in Figure 10C. As can be seen, the molar ratio of Cd and Se in QD-1 under different incubation concentrations showed no significant difference but they were significantly lower than that in the original NH_2-625 QDs. Speciation of QDs in HepG2 cells incubated with other three QDs were analyzed by

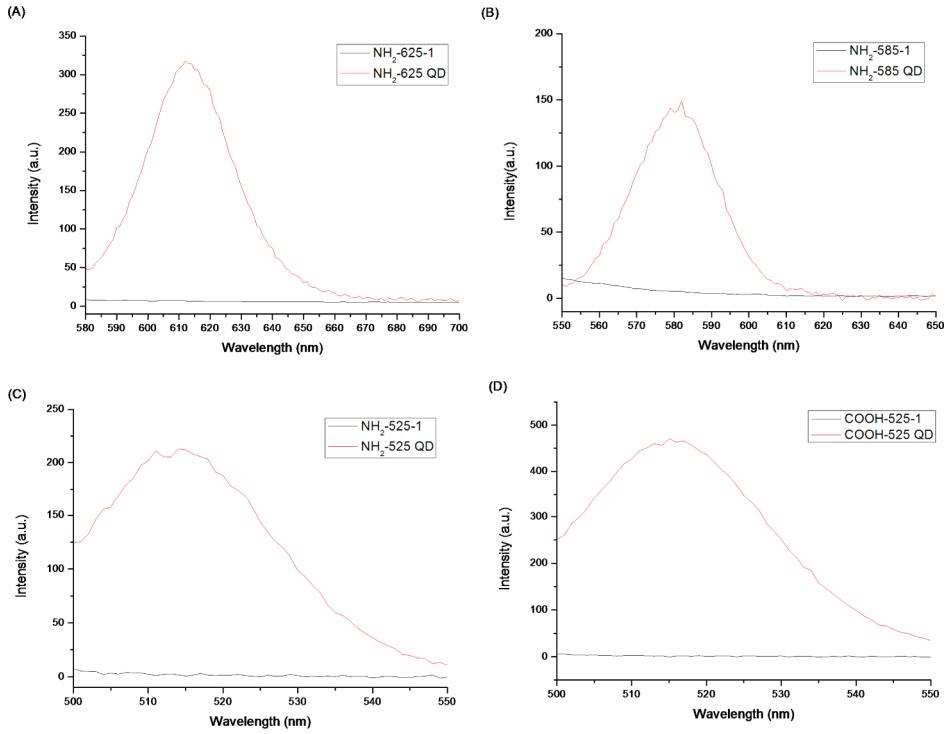

Figure 7. Fluorescence emission curve of QD-1 and original QDs. (A) NH_2-625; (B) NH_2-585; (C) NH_2-525; (D) COOH-525.

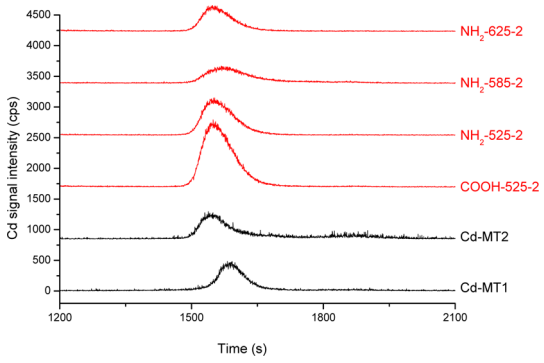

Figure 8. Retention performance of QD-2 and Cd-MT1, Cd-MT2 obtained by SEC-ICP-MS.

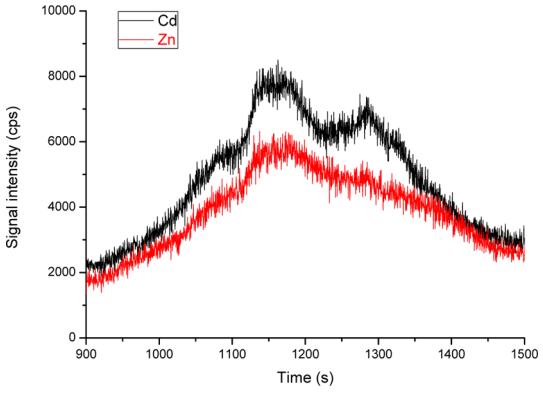

Figure 9. Retention performance of NH_2-625-2 obtained by RPLC-ICP-MS.

the same method. Similar results were found as shown in Figure S2−S4.

Speciation of CdSe/ZnS QDs in HepG2 Cells Incubated for Different Times. HepG2 cells were incubated with four CdSe/ZnS QDs for different time (6, 12, 24 h), and the speciation of QDs were analyzed by SEC-ICP-MS. As shown in Figure 11A, only QD-1 and QD-2 were detected in HepG2 cells incubated with NH_2-625 QDs for different time. Their amount both increased with the increase of incubation time by determining Cd. The results obtained by Se detection (Figure 11B) exhibited similar tendency for QD-1. Meanwhile, the molar ratio of Cd and Se in QD-1 was determined by ICP-MS, and the results are shown in Figure 11C. The molar ratio of Cd and Se decreased with the increase of the incubation time and was much lower than that in original NH_2-625 QDs. The same tendency was found for other three QDs group (Figure S5−S7). The decrease of molar ratio of Cd and Se in QD-1 with the extending of incubation time might be caused by the continuous decomposition of QDs under acidic environment. To verify the assumption, the release of Cd and Se from QDs was simulated in acidic buffer solution (pH 5.0). The results in Figure 12 showed an increasing release of Cd and Se from QDs with time prolonged. Meanwhile, molar ratio of Cd and Se released from NH_2-625 QDs was found to be larger than that in the original NH_2-625 QD (1.4) and further increased with incubation time (Figure 12A). This suggested a faster release of Cd than Se from CdSe/ZnS QDs under acidic environment.

Speciation of CdSe/ZnS QDs in HepG2 Cells at Different Elimination Times. The speciation of QDs in HepG2 cells

TABLE 1. Metallothioneins Information of NH_2-625-2 at 1170s

Apo-MTs				MTs			
m/z, *z* = 4, most abundant				*m/z*, *z* = 5, most abundant			
measured	theoretical	difference, ppm	compound	measured	theoretical	difference, ppm	compound
1521.8024	1521.8101	−5.0	N Ac-MT2a	1363.0851	1363.0973	−9.0	Cd_6Zn−N Ac-MT2a
				1353.4984	1353.5021	−2.8	Cd_5Zn_2−N Ac-MT2a
1528.3068	1528.3140	−4.7	MT1m	1368.2872	1368.3005	−9.7	Cd_6Zn−MT1m
				1358.6931	1358.7052	−8.7	Cd_5Zn_2−MT1m

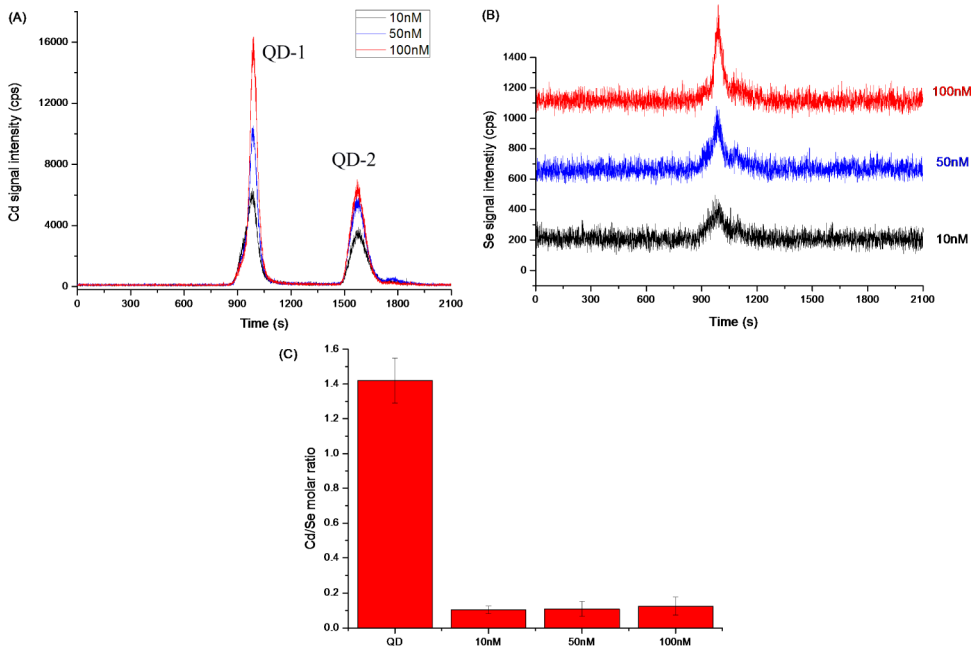

Figure 10. Speciation of QDs in HepG2 cells incubated with different concentrations of NH_2-625 QD. (A) Cd signal obtained by SEC-ICP-MS; (B) Se signal obtained by SEC-ICP-MS. (C) Cd/Se molar ratio in NH_2-625-1 determined by PN-ICP-MS.

under different elimination time was analyzed by SEC-ICP-MS. As shown in Figure 13A, only two kinds of species, QD-1 and QD-2, were found in HepG2 cells incubated with NH_2-625 QD for different elimination time (0, 12, 24, 48 h). The amount of Cd in QD-1 decreased with the increase of the elimination time and the same tendency was found in Figure 13B by determining Se. However, QD-2 presented a different tendency, the signal of Cd increased first in the elimination time range of 0−12 h and then decreased in the time range of 12−48 h. Speciation of QDs in HepG2 cells incubated with other three QDs was analyzed by the same method. The variation tendency of QD-1 and QD-2 in NH_2-525 QDs group (Figure S8) and COOH-525 QDs group (Figure S9) were the same as that in NH_2-625 QDs group. However, the result of NH_2-585 QDs group (Figure S10) showed a little different tendency and the amount of QD-1 and QD-2 both decreased at the range of 0−48 h. Further investigation will be processed for the understanding of the performance difference.

DISCUSSION

Biosafety of QDs has been becoming one of the research hotspots over the past decade due to their potential application in clinical medicine.[32−34] It is well-known many factors can affect the toxicity of QDs. Among them, the transformation and species of QDs in biological systems cannot be neglected.[16,17] While, little is known about the existing form of QDs in living cells so far. In this work, we focused on the speciation of CdSe/ZnS QDs in HepG2 cells for the first time. Two species (QD-1 and QD-2) were found in the HepG2 cells incubated with four CdSe/ZnS QDs by using SEC-ICP-MS measurement, and they were considered to be transformed by the cellular ingested QDs because no signals of Cd and Se were found in the control group. What's more, in our previous study,[35] the employed QDs was proved to be very stable in physiological conditions and no free Cd released from QDs was observed. Accordingly, the observed species herein are due to the intracellular processing of the QDs instead the decomposition of QDs under

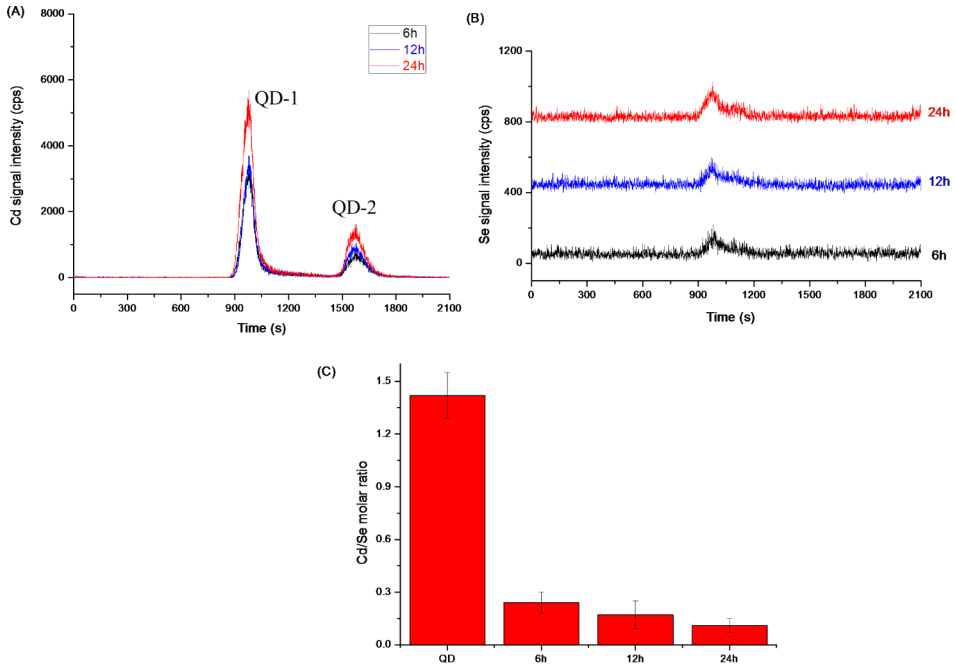

Figure 11. Speciation of QDs in HepG2 cells after incubated with NH_2-625 QD for different time. (A) Cd signal obtained by SEC-ICP-MS; (B) Se signal obtained by SEC-ICP-MS; (C) Cd/Se molar ratio in NH_2-625-1 determined by PN-ICP-MS.

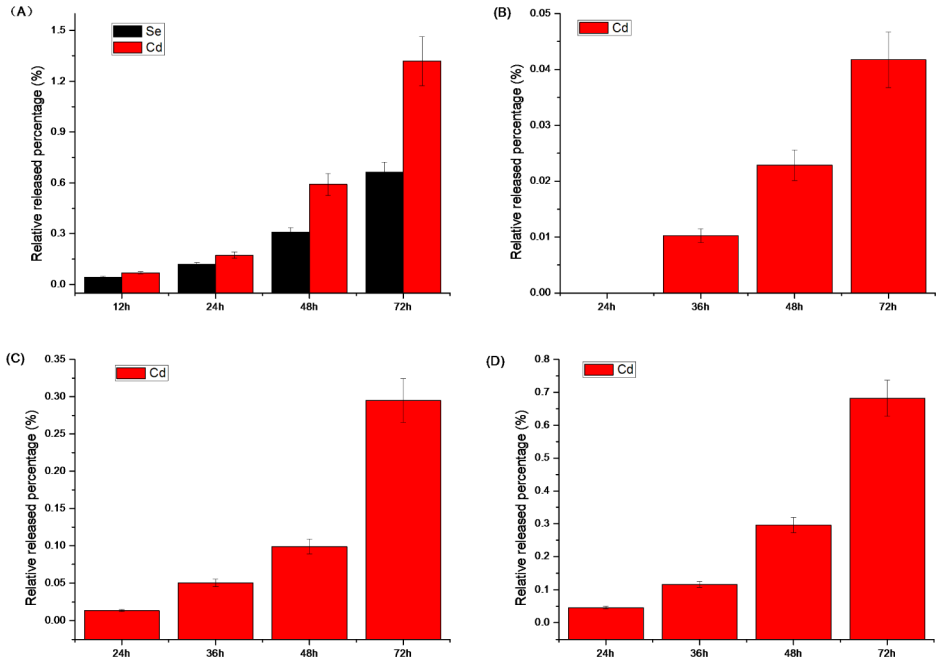

Figure 12. Release of Cd and Se from QDs in buffer solution. (A) NH_2-625; (B) NH_2-585; (C) NH_2-525; (D) COOH-525.

physiological conditions. Meanwhile, the ingested QDs in HepG2 cells mainly existed as QD-1 and QD-2, occupied appr. 70% of the total QDs uptaken by cells and no small complex, such as Cd-EDTA, were found. Besides QD-1 and QD-2, there might be some other metabolic products of QDs, like several Se-containing species, which is probably caused by the release of Se together with Cd from the QDs surface in cells. However, their amount is less than 30% of the total QDs uptaken by cells. They were undetected by the employed SEC-ICP-MS method possibly because their amount was lower than the detection limit of this method.

The structure of QD-1 and QD-2 were preliminarily characterized by a series of techniques. The TEM characteristic result showed QD-1 was a kind of nanoparticles with similar size to original QDs, while ICP-MS results showed a different molar ratio of Cd and Se for QD-1 and original QDs. The t_R of QD-1 was close to that of CdSe/ZnS QDs, suggesting a similar retention

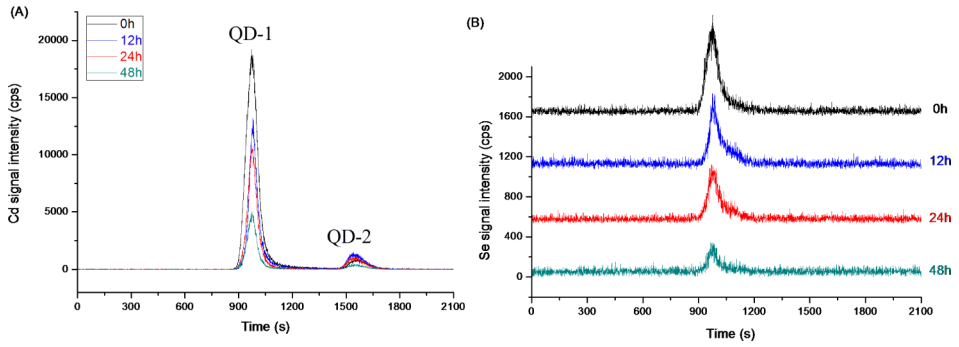

Figure 13. Speciation of QDs in HepG2 cells incubated with NH_2-625 QD at different elimination time. (A) Cd signal by SEC-ICP-MS; (B) Se signal by SEC-ICP-MS.

behavior to CdSe/ZnS QDs. Though no obvious fluorescence signal was detected for QD-1, it is hard to exclude that QD-1 inherits fluorescence properties because obvious fluorescence was observed for four CdSe/ZnS QDs in lysosomes of HepG2 cells after incubation for 24 h in our previous work.[35] Thus, we speculated the original QDs were included in QD-1. The possible reasons for that the fluorescence of QD-1 was not observed could be attributed to the following facts. First, the fluorescence intensity of QD-1 was too low to be detected by the employed fluorescence spectrophotometer. The amount of QD-1 was very low in the incubated cells, partly due to the low uptake efficiency of QDs by HepG2 cells as reported in our previous study.[35] Meanwhile, the coexisting protein in the fraction of QD-1 might interfere the detection of the QD-1 fluorescence emission. Thus, QD-1 was ultimately defined as a kind of QD-like nanoparticles, which might contain both original and degraded QDs and its detail and accurate composition needs further study.

QD-2 was confirmed to be a kind of Cd-MTs by parallel RPLC-ICP-MS/ESI-Q-TOF-MS analysis. The formation of Cd-MTs was the combination of Cd ions released from the CdSe/ZnS QDs and the MTs in the cells. It is well-known that ZnS surface coating can prevent the release of Cd from CdSe QDs core and ultimately the toxicity of CdSe QDs.[36,37] However, whether the surface coating can completely prevent the release of toxic components from QDs under the complicated environmental and biological conditions is still a question. The stability of QDs is challenged in the end-up location of lysosomal compartments, which is an acidic and oxidative environment.[11,38] Several studies have reported the release of Cd from CdSe QDs under the protection coating.[16,39,40] Similarly, in the present study, the increased release of Cd and Se from CdSe/ZnS QDs with time was found under acidic solution (pH 5.0). The released Cd was considered to be bound to MTs, a kind of small, sulfydryl-rich, metal-binding protein.[41,42] As reported in previous studies, MTs played a key role on the protection of cells from the Cd toxicity.[42−45] In our previous study, the overexpression of MT-related gene was found in HepG2 cells incubated with all four kinds of CdSe/ZnS QDs.[35]

The cellular uptake and elimination of CdSe/ZnS QDs has been studied from an insight of total amount of intracellular QDs in our previous study,[35] and it should be pointed out that no evident cytotoxicity of four employed QDs was observed in the range of 10−100 nM, which might be attributed to the structure of the ZnS shell and the PEG coating in four QDs. In this work, a further study based on speciation of the ingested QDs by HepG2 cells was carried out. Our results showed only two kinds of species, QD-1 and QD-2, were found under all the conditions, including different incubation concentrations, incubation time and elimination time. However, the amount of QD-1 and QD-2 varied under different incubation conditions. The amount of QD-1 and QD-2 both increased with the increase of incubation concentrations for all four kinds of CdSe/ZnS QDs. The amount of QD-1 and QD-2 depended on the cellular uptake of QDs which were found to be increasing with the incubation concentrations increased.[35] Thus, a corresponding increase of QD-1 and QD-2 was expected. A similar result was found under different incubation time. QD-1 and QD-2 both increased with time due to the uptake of QDs increased with time. However, a decreased molar ratio of Cd/Se in QD-1 was found over incubation time. This might be caused by the further decomposition of QD-1. As a faster release of Cd from NH_2-625 QD than Se was found under acidic solution, the further decompose of QD-1 in cells might cause more release of Cd and ultimately a decreased molar ratio of Cd/Se with time.

Meanwhile, the variation in the amount of QD-1 and QD-2 at different elimination time was investigated. The results showed that the amount of QD-1 decreased with time, but QD-2 increased first and then decreased. The amount of QD-1 was influenced by two factors: the elimination by cells and the further self-decomposition. the These two factors both decreased the amount of QD-1 and ultimately caused the decrease of QD-1 with elimination time. The amount of QD-2 was affected by two factors: the elimination by cells which decreased the amount of QD-2 and the contribution of QD-1

further self-decomposition which increased the amount of QD-2. The ultimate tendency depended on the net effect of these two factors. At the beginning of elimination, the contribution of QD-1 self-decomposition played a leading role and ultimately increased the amount of QD-2. As time extended, elimination by cells played a more important role and ultimately decreased the amount of QD-2. The results in NH_2-585 QDs group showed a little difference compared with other three QDs group and the amount of QD-2 kept decreasing over time. This might be caused by the slow degradation of NH_2-585 QDs for which the released Cd signal was detected until 36 h (Figure 12). As the self-decomposition of QD-1 was slow and even can be ignored, the net amount of QD-2 mainly was depended on the cellular elimination and ultimately decreased over time.

CONCLUSION

In summary, speciation of four CdSe/ZnS QDs in HepG2 cells was processed by ICP-MS-based hyphenated techniques. After incubation by four CdSe/ZnS QDs with different functional groups (NH_2 or COOH) and particle sizes under various concentrations for different times, respectively, two kinds of chemical form, named as QD-1 and QD-2, were found in HepG2 cells. QD-1 and QD-2 were confirmed to be a kind of QD-like nanoparticles and a kind of Cd-MTs, respectively. This work provided valuable information on the speciation of CdSe/ZnS QDs in HepG2 cells for the first time and the investigation and verification of these two species of QDs were carried out with the cooperative aid of inorganic and organic mass spectrometry-based hyphenated techniques, which contributes to understanding the metabolism and toxicity of QDs in living cells.

MATERIALS AND METHODS

Reagents and Instruments. The four CdSe/ZnS QDs used in this study (NH_2-625, NH_2-585, NH_2-525 and COOH-525) were composed of cadmium selenide (CdSe) core and zinc sulfide (ZnS) shell particles, encapsulated within the same amphipathic polymer of poly(acrylic acid) and PEG coating. The difference between them was the surface functional group (NH_2 or COOH) and the maximum emission wavelength (525, 585, and 625 nm), and their detail physicochemical properties were described previously.[35] The standard stock solutions of Cd (1 g/L) and Se (1 g/L) were prepared by dissolving $Cd(NO_3)_2 \cdot 4H_2O$ (AR, Shanghai Chemistry Reagent Company, China) and Na_2SeO_3 (97%, Wako, Japan) in high purity deionized water, respectively. LC−MS grade reagents such as ammonium acetate (NH_4Ac), trifluoroacetic acid (TFA) and CH_3OH were purchased from Anaqua Chemicals Supply Inc. (America). Zn-MT1 and Zn-MT2 (>97%, from rabbit liver) were purchased from Dalian Free Trade Zone United BoTai Biotechnology Co., Ltd. (Dalian, China). Cd-MT1 and Cd-MT2 used in this study were obtained by replacing Zn in Zn-MT1 and Zn-MT2 with Cd ion, respectively. All other reagents were at least of analytical reagent grade. To control the blank value, all the laboratory ware was thoroughly washed by soaking in 10% HNO_3 for at least 24 h. The sub-boiled HNO_3 was employed throughout the experiments.

The transmission electron micrograph (TEM) was obtained using a JEOL EM2010 electron microscope (Tokyo, Japan). The sample was lyophilized by a vacuum freezing dryer (Beijing, China). A hemacytometer (Shanghai Qiujing Biochemical Reagent Instrument Co., Ltd., China) was used for cell counting. The sonicator (40KW, XinZi Tech, Ningbo, China) was used for cell rapture.

Cellular Culture and Coincubation with CdSe/ZnS QDs. Human hepatocellular carcinoma cells (HepG2) were cultured in Dulbecco's modified Eagle's medium (DMEM, Gibco) supplemented with 10% fetal bovine serum (Gibco) and 1% penicillin/streptomycin at 37 °C in a humidified atmosphere with 5% CO_2. The medium was renewed every other day, and cells were passaged when they reached 80% confluence. Before being exposed to QDs, HepG2 cells were seeded in 25 cm^2 flasks (Corning, NY, USA) and cultured at 37 °C overnight. All the QD solution was freshly suspended in DMEM solution without serum before cell culture treatment.

Cell Sample Treatment. After incubation, the cells was washed with cold phosphate buffer saline (PBS) for three times and harvested by trypsinization. Then cells were redispersed in 600 μL 20 mM ammonium acetate (pH 7.4), and the solution was ultrasonicated in ice−water bath for 30 min (power 50%, 30 s stop, 30 s pulse). The mixture was centrifuged (4 °C, 8000*g*, 10 min) and the supernatant was collected and stored at 4 °C before analysis.

SEC-ICP-MS Measurement. The obtained cytosol as mentioned above was filtered with 0.22 μm filter membrane prior to analysis and an aliquot of 50 μL was subjected to SEC-ICP-MS measurement. In details, sample separation was carried out on a LC-10AD HPLC system (Shimadzu, Japan) equipped with a size exclusion column (Superdex 75 10/300 GL, 300 × 10 mm I.D., 13 μm, GE Healthcare, Sweden). The effluent was directly infused into ICP-MS (Agilent 7500a, Japan) for detection. The operation conditions of SEC-ICP-MS method are summarized in Table S1.

Pneumatic Nebulization (PN)-ICP-MS Measurement of QDs, QD-1 and QD-2. HepG2 cells were incubated with QDs (100 nM) for 24 h. After incubation, the cells was washed with PBS solution for three times and harvested by trypsinization. The collected cells were divided into two equal parts. One part was directly digested by concentrated nitric acid and determined by PN-ICP-MS, and the result was considered as the total amount of QDs in the cells. The other part was ultrasonicated in ice−water bath for 30 min and the supernatant was collected after centrifugation. Then, the collected supernatant was separated by SEC column after filtration and the fraction of QD-1 (840−1100 s) and QD-2 (1450−1700 s) were collected, respectively. Then, these two fractions solution were mixed together and digested with concentrated nitric acid and determined by PN-ICP-MS, the result was considered as the total amount of QD-1 and QD-2 in the cells.

Comparison of Retention Time. In order to investigate the molecular weight of QD-1 and QD-2, the retention time of four kinds of CdSe/ZnS QDs and two kinds of metallothionein (Cd-MT1 and Cd-MT2, 6−7KDa) were determined by SEC-ICP-MS. The retention time of cadmium-ethylenediamine tetraacetic acid complex (Cd-EDTA) was 1860 s according to ICP-MS determination. The retention time of Bovine Serum Albumin (BSA, 67KDa) was 1134s determined by UV detection after SEC separation.

Molar Ratio of Cd/Se in QD-1 Determined by PN-ICP-MS. The QD-1 fraction (840−1100 s) was collected after separation by SEC column as described above and then digested with concentrated HNO_3 (67%) for 3 h at 85 °C. The solution was evaporated to remove superfluous acid and diluted with 5% HNO_3 to 1 mL prior to PN-ICP-MS determination.

Fluorescence Detection. The QD-1 fraction (840−1100 s) was collected after separation by SEC column as described above. Then the fluorescence spectra of QD-1 was obtained with a RF-5301PC spectrophotometer (Shimadzu, Japan) equipped with a 150 W xenon lamp (Ushio Inc., Japan). Meanwhile, the fluorescence spectra of four CdSe/ZnS QDs solution were obtained by the same process.

Cd and Se Released from QD Determined by PN-ICP-MS. The possible degradation of QDs in cells was investigated in PBS buffer (pH 5.0). 200 μL of 100 nmol L^{-1} QDs were dispersed and incubated in PBS buffer solution at 37 °C for a certain time. Then the mixed solution was ultrafiltrated (4 °C, 10000*g*, 10 min) with centrifugal filter devices (amicon ultra-4, 3 kDa, Millipore, USA). The ultrafiltrate was collected and subjected to PN-ICP-MS detection of Cd and Se. The total amount of Cd and Se in QDs without incubation was also determined to calculate the release percentage of Cd and Se.

RPLC-ICP-MS/ESI-QTOF-MS Measurement. The QD-2 fraction (1450−1700 s) was collected from ten injections (50 μL per injection). Then the fractions were combined together, freeze-dried, resolubilized in 50 μL of water and stored in −70 °C before subsequent detection. Aliquot of 30 μL sample was subjected to RPLC-ICP-MS/ESI-MS analysis. In details, sample separation was carried out on a ultimate 3000 HPLC system (Dionex, USA) equipped with a C_{18} column acclaim 120 (150 × 2.1 mm I.D., 3 μm, Dionex, USA). The effluent was directly infused into a zero dead volume PEEK T-piece with a compensated current (H_2O or 1% TFA) delivered by means of a micro pump in the Dionex HPLC system. The confluence solution was then infused into a splitter. The splitter was simultaneously coupled with an X series2 ICP-MS (ThermoFisher Scientific, USA) with a concentrated nebulizer and a microTOF-Q III MS with an ESI ion source (Bruker, Germany), with a split ratio of 50:1 (effluent to ICP-MS/effluent to ESI-Q-TOF-MS). The operation conditions of C_{18} HPLC-ICP-MS/ESI-Q-TOF-MS are listed in Table S2. The initial calibration of ESI-Q-TOF-MS was performed using sodium trifluoroacetate. The data were analyzed by Compass Data Analysis software (Bruker, Germany). The information on human MTs, MT2a (UniProtKB: P02795) and MT1m (UniProtKB: Q8N339), were obtained from Uniprot database. The amino acid sequences of MT2a and MT1m were 1′ MDPNCSCAAGDSCTCAGSCKCKECKCTSCKKSCCSCCPVGCAKCAQGCICKGASDKCSCCA 61′ and 1′ MDPNCSCTTGVSCACTGSCTCKECKCTSCKKSCCSCCPVGCAKCAHGCVCKGTLENCSCCA 61′, respectively. The acetylated site of MT2a was on the unique methionine at N-terminal (1′). The mass-to-charge ratio in theory ($m/z_{theoretical}$) was obtained from IsotopePattern software (Bruker, Germany) and the mass accuracy was expressed in ppm and calculated as the ratio $(m/z_{measured} - m/z_{theoretical})/m/z_{theoretical}$ multiplied by 10^6.

Speciation of QDs in HepG2 Cells by SEC-ICP-MS under Different Incubation Conditions. To analyze the species of QDs in HepG2 cells under different incubation conditions, HepG2 cells were incubated with QDs under a series of incubation concentrations (10, 50, 100 nM), incubation time (6, 12, 24 h) and elimination time (0, 12, 24, 48 h), respectively. The sample treatment and analytical procedure were referred to the process as described above.

Conflict of Interest: The authors declare no competing financial interest.

Acknowledgment. The authors would like to thank Professors Daiwen Pang and Zhiling Zhang for their technical assistance in cell culture. This work is financially supported by the National Basic Research Program of China (973 Program, 2013CB933900), the National Nature Science Foundation of China (Nos. 21175102, 21075095, 21205090, 21375097, 21575107), the Science Fund for Creative Research Groups of NSFC (Nos. 20621502, 20921062) and the Fundamental Research Funds for the Central Universities (114009).

Supporting Information Available: The Supporting Information is available free of charge on the ACS Publications website at DOI: 10.1021/acsnano.5b04365.

Supporting tables and figures. (PDF)

REFERENCES AND NOTES

1. Ye, F.; Barrefelt, A.; Asem, H.; Abedi-Valugerdi, M.; El-Serafi, I.; Saghafian, M.; Abu-Salah, K.; Alrokayan, S.; Muhammed, M.; Hassan, M. Biodegradable Polymeric Vesicles Containing Magnetic Nanoparticles, Quantum Dots and Anticancer Drugs for Drug Delivery and Imaging. *Biomaterials* **2014**, *35*, 3885–3894.
2. Rakovich, T. Y.; Mahfoud, O. K.; Mohamed, B. M.; Prina-Mello, A.; Crosbie-Staunton, K.; Van den Broeck, T.; De Kimpe, L.; Sukhanova, A.; Baty, D.; Rakovich, A.; *et al.* Highly Sensitive Single Domain Antibody-Quantum Dot Conjugates for Detection of HER2 Biomarker in Lung and Breast Cancer Cells. *ACS Nano* **2014**, *8*, 5682–5695.
3. Chu, M. Q.; Pan, X. J.; Zhang, D.; Wu, Q.; Peng, J. L.; Hai, W. X. The Therapeutic Efficacy of CdTe and CdSe Quantum Dots for Photothermal Cancer Therapy. *Biomaterials* **2012**, *33*, 7071–7083.
4. Yan, M.; Zhang, Y.; Xu, K. D.; Fu, T.; Qin, H. Y.; Zheng, X. X. An *in Vitro* Study of Vascular Endothelial Toxicity of CdTe Quantum Dots. *Toxicology* **2011**, *282*, 94–103.
5. Luo, Y. H.; Wu, S. B.; Wei, Y. H.; Chen, Y. C.; Tsai, M. H.; Ho, C. C.; Lin, S. Y.; Yang, C. S.; Lin, P. P. Cadmium-Based Quantum Dot Induced Autophagy Formation for Cell Survival *via* Oxidative Stress. *Chem. Res. Toxicol.* **2013**, *26*, 662–673.
6. Nagy, A.; Steinbruck, A.; Gao, J.; Doggett, N.; Hollingsworth, J. A.; Iyer, R. Comprehensive Analysis of the Effects of CdSe Quantum Dot Size, Surface Charge, and Functionalization on Primary Human Lung Cells. *ACS Nano* **2012**, *6*, 4748–4762.
7. Fang, T. T.; Li, X.; Wang, Q. S.; Zhang, Z. J.; Liu, P.; Zhang, C. C. Toxicity Evaluation of CdTe Quantum Dots with Different Size on Escherichia Coli. *Toxicol. In Vitro* **2012**, *26*, 1233–1239.
8. Hoshino, A.; Fujioka, K.; Oku, T.; Suga, M.; Sasaki, Y. F.; Ohta, T.; Yasuhara, M.; Suzuki, K.; Yamamoto, K. Physicochemical Properties and Cellular Toxicity of Nanocrystal Quantum Dots Depend on Their Surface Modification. *Nano Lett.* **2004**, *4*, 2163–2169.
9. Clift, M. J. D.; Varet, J.; Hankin, S. M.; Brownlee, B.; Davidson, A. M.; Brandenberger, C.; Rothen-Rutishauser, B.; Brown, D. M.; Stone, V. Quantum Dot Cytotoxicity *in Vitro*: An Investigation into the Cytotoxic Effects of a Series of Different Surface Chemistries and Their Core/Shell Materials. *Nanotoxicology* **2011**, *5*, 664–674.
10. Rivera-Gil, P.; De Aberasturi, D. J.; Wulf, V.; Pelaz, B.; Del Pino, P.; Zhao, Y. Y.; De La Fuente, J. M.; De Larramendi, I. R.; Rojo, T.; Liang, X. J.; *et al.* The Challenge to Relate the Physicochemical Properties of Colloidal Nanoparticles to Their Cytotoxicity. *Acc. Chem. Res.* **2013**, *46*, 743–749.
11. Derfus, A. M.; Chan, W. C. W.; Bhatia, S. N. Probing the Cytotoxicity of Semiconductor Quantum Dots. *Nano Lett.* **2004**, *4*, 11–18.
12. Su, Y. Y.; Hu, M.; Fan, C. H.; He, Y.; Li, Q. N.; Li, W. X.; Wang, L. H.; Shen, P. P.; Huang, Q. The Cytotoxicity of CdTe Quantum Dots and the Relative Contributions from Released Cadmium Ions and Nanoparticle Properties. *Biomaterials* **2010**, *31*, 4829–4834.
13. Li, K. G.; Chen, J. T.; Bai, S. S.; Wen, X.; Song, S. Y.; Yu, Q.; Li, J.; Wang, Y. Q. Intracellular Oxidative Stress and Cadmium Ions Release Induce Cytotoxicity of Unmodified Cadmium Sulfide Duantum Dots. *Toxicol. In Vitro* **2009**, *23*, 1007–1013.
14. Albanese, A.; Chan, W. C. W. Effect of Gold Nanoparticle Aggregation on Cell Uptake and Toxicity. *ACS Nano* **2011**, *5*, 5478–5489.
15. Liu, J. Y.; Wang, Z. Y.; Liu, F. D.; Kane, A. B.; Hurt, R. H. Chemical Transformations of Nanosilver in Biological Environments. *ACS Nano* **2012**, *6*, 9887–9899.
16. Mahendra, S.; Zhu, H. G.; Colvin, V. L.; Alvarez, P. J. Quantum Dot Weathering Results in Microbial Toxicity. *Environ. Sci. Technol.* **2008**, *42*, 9424–9430.
17. Pettibone, J. M.; Gigault, J.; Hackley, V. A. Discriminating the States of Matter in Metallic Nanoparticle Transformations: What Are We Missing? *ACS Nano* **2013**, *7*, 2491–2499.
18. George, S.; Lin, S. J.; Jo, Z. X.; Thomas, C. R.; Li, L. J.; Mecklenburg, M.; Meng, H.; Wang, X.; Zhang, H. Y.; Xia, T.; *et al.* Surface Defects on Plate-Shaped Silver Nanoparticles Contribute to Its Hazard Potential in a Fish Gill Cell Line and Zebrafish Embryos. *ACS Nano* **2012**, *6*, 3745–3759.

19. Metz, K. M.; Mangham, A. N.; Bierman, M. J.; Jin, S.; Hamers, R. J.; Pedersen, J. A. Engineered Nanomaterial Transformation under Oxidative Environmental Conditions: Development of an *in Vitro* Biomimetic Assay. *Environ. Sci. Technol.* **2009**, *43*, 1598–1604.
20. Wiecinski, P. N.; Metz, K. M.; Heiden, T. C. K.; Louis, K. M.; Mangham, A. N.; Hamers, R. J.; Heideman, W.; Peterson, R. E.; Pedersen, J. A. Toxicity of Oxidatively Degraded Quantum Dots to Developing Zebrafish (Danio rerio). *Environ. Sci. Technol.* **2013**, *47*, 9132–9139.
21. Soenen, S. J.; Abe, S.; Manshian, B. B.; Aubert, T.; Hens, Z.; De Smedt, S. C.; Braeckmans, K. The Effect of Intracellular Degradation on Cytotoxicity and Cell Labeling Efficacy of Inorganic Ligand-Stabilized Colloidal CdSe/CdS Quantum Dots. *J. Biomed. Nanotechnol.* **2015**, *11*, 631–643.
22. Beyersmann, D.; Hartwig, A. Carcinogenic Metal Compounds: Recent Insight into Molecular and Cellular Mechanisms. *Arch. Toxicol.* **2008**, *82*, 493–512.
23. Haraguchi, H. Metallomics as Integrated Biometal Science. *J. Anal. At. Spectrom.* **2004**, *19*, 5–14.
24. Shi, W.; Chance, M. R.; Metallomics and Metalloproteomics. *Cell. Mol. Life Sci.* **2008**, *65*, 3040–3048.
25. Mounicou, S.; Szpunar, J.; Lobinski, R. Metallomics: The Concept and Methodology. *Chem. Soc. Rev.* **2009**, *38*, 1119–1138.
26. Wang, B.; Feng, W. Y.; Zhao, Y. L.; Chai, Z. F. Metallomics Insights for *in Vivo* Studies of Metal Based Nanomaterials. *Metallomics* **2013**, *5*, 793–803.
27. Li, Y. F.; Gao, Y. X.; Chai, Z. F.; Chen, C. Y. Nanometallomics: An Emerging Field Studying the Biological Effects of Metal-Related Nanomaterials. *Metallomics* **2014**, *6*, 220–232.
28. Owens, S. A.; Carpenter, M. C.; Sonne, J. W. H.; Miller, C. A.; Renehan, J. R.; Odonkor, C. A.; Henry, E. M.; Miles, D. T. Reversed-Phase HPLC Separation of Water-Soluble, Monolayer-Protected Quantum Dots. *J. Phys. Chem. C* **2011**, *115*, 18952–18957.
29. Al-Somali, A. M.; Krueger, K. M.; Falkner, J. C.; Colvin, V. L. Recycling Size Exclusion Chromatography for the Analysis and Separation of Nanocrystalline Gold. *Anal. Chem.* **2004**, *76*, 5903–5910.
30. Helfrich, A.; Bruchert, W.; Bettmer, J. Size Characterisation of Au Nanoparticles by ICP-MS Coupling Techniques. *J. Anal. At. Spectrom.* **2006**, *21*, 431–434.
31. Knoppe, S.; Boudon, J.; Dolamic, I.; Dass, A.; Burgi, T. Size Exclusion Chromatography for Semipreparative Scale Separation of Au-38(SR)(24) and Au-40(SR)(24) and Larger Clusters. *Anal. Chem.* **2011**, *83*, 5056–5061.
32. Yong, K. T.; Law, W. C.; Hu, R.; Ye, L.; Liu, L. W.; Swihart, M. T.; Prasad, P. N. Nanotoxicity Assessment of Quantum dots: From Cellular to Primate Studies. *Chem. Soc. Rev.* **2013**, *42*, 1236–1250.
33. Winnik, F. M.; Maysinger, D. Quantum Dot Cytotoxicity and Ways to Reduce It. *Acc. Chem. Res.* **2013**, *46*, 672–680.
34. Tsoi, K. M.; Dai, Q.; Alman, B. A.; Chan, W. C. W. Are Quantum Dots Toxic? Exploring the Discrepancy Between Cell Culture and Animal Studies. *Acc. Chem. Res.* **2013**, *46*, 662–671.
35. Peng, L.; He, M.; Chen, B. B.; Wu, Q. M.; Zhang, Z. L.; Pang, D. W.; Zhu, Y.; Hu, B. Cellular Uptake, Elimination and Toxicity of CdSe/ZnS Quantum Dots in HepG2 Cells. *Biomaterials* **2013**, *34*, 9545–9558.
36. Kirchner, C.; Liedl, T.; Kudera, S.; Pellegrino, T.; Javier, A. M.; Gaub, H. E.; Stolzle, S.; Fertig, N.; Parak, W. J. Cytotoxicity of Colloidal CdSe and CdSe/ZnS Nanoparticles. *Nano Lett.* **2005**, *5*, 331–338.
37. Su, Y. Y.; He, Y.; Lu, H. T.; Sai, L. M.; Li, Q. N.; Li, W. X.; Wang, L. H.; Shen, P. P.; Huang, Q.; Fan, C. H. The Cytotoxicity of Cadmium Based, Aqueous Phase - Synthesized, Quantum Dots and Its Modulation by Surface Coating. *Biomaterials* **2009**, *30*, 19–25.
38. Soenen, S. J.; Demeester, J.; De Smedt, S. C.; Braeckmans, K. The Cytotoxic Effects of Polymer-Coated Quantum Dots and Restrictions for Live Cell Applications. *Biomaterials* **2012**, *33*, 4882–4888.
39. Corazzari, I.; Gilardino, A.; Dalmazzo, S.; Fubini, B.; Lovisolo, D. Localization of CdSe/ZnS Quantum Dots in the Lysosomal Acidic Compartment of Cultured Neurons and Its Impact on Viability: Potential Role of Ion Release. *Toxicol. In Vitro* **2013**, *27*, 752–759.
40. Soenen, S. J.; Montenegro, J. M.; Abdelmonem, A. M.; Manshian, B. B.; Doak, S. H.; Parak, W. J.; De Smedt, S. C.; Braeckmans, K. The Effect of Nanoparticle Degradation on Poly(methacrylic acid)-Coated Quantum Dot Toxicity: The Importance of Particle Functionality Assessment in Toxicology. *Acta Biomater.* **2014**, *10*, 732–741.
41. Coyle, P.; Philcox, J. C.; Carey, L. C.; Rofe, A. M. Metallothionein: The Multipurpose Protein. *Cell. Mol. Life Sci.* **2002**, *59*, 627–647.
42. Babula, P.; Masarik, M.; Adam, V.; Eckschlager, T.; Stiborova, M.; Trnkova, L.; Skutkova, H.; Provaznik, I.; Hubalek, J.; Kizek, R. Mammalian Metallothioneins: Properties and Functions. *Metallomics* **2012**, *4*, 739–750.
43. Chiaverini, N.; De Ley, M. Protective Effect of Metallothionein on Oxidative Stress-Induced DNA Damage. *Free Radical Res.* **2010**, *44*, 605–613.
44. Urani, C.; Melchioretto, P.; Canevali, C.; Crosta, G. F. Cytotoxicity and Induction of Protective Mechanisms in HepG2 Cells Exposed to Cadmium. *Toxicol. In Vitro* **2005**, *19*, 887–892.
45. Klaassen, C. D.; Liu, J.; Diwan, B. A. Metallothionein Protection of Cadmium Toxicity. *Toxicol. Appl. Pharmacol.* **2009**, *238*, 215–220.